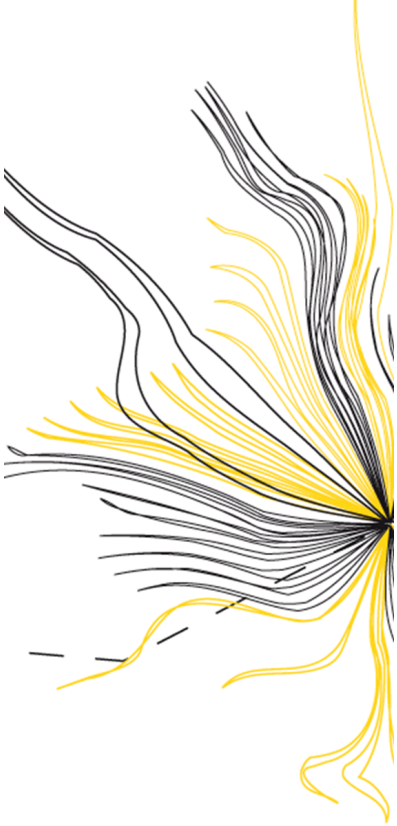

UNIVERSITY OF TWENTE.

Faculty of Electrical Engineering,
Mathematics and Computer Science

Plant and Controller Co-optimization for an Active Vibration Isolation System Using Convexified LMIs

Master Thesis Systems & Control

G.H.W. Schrijver

July 2023

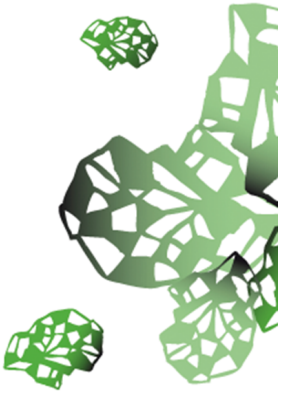

Examination committee:
dr.ir. W.B.J. Hakvoort
dr. H. Koroglu
ir. S.T. Spanjer
dr.ir. G. Meinsma

Precision Engineering
Faculty of Engineering Technologies
University of Twente
P.O. Box 217
7500 AE Enschede
The Netherlands

Summary

The common methodology for system design is to determine specifications for the plant and the controller and optimize them independently. Although the plant and controller may be optimal for their respective design specifications, the independent design may lead to a sub-optimal closed loop system. Simultaneous design of the plant and controller can be considered to obtain an optimal solution but this is in general a nonlinear problem and convexity is not guaranteed. Several works have addressed plant and controller co-optimization, often resulting in an iterative approach. In this work plant, and controller co-optimization is investigated in a linear matrix inequality framework. The use of so-called convexifying potentials is adopted to locally linearize the problem. These approximations are then used to iteratively approach a stationary point in the plant and controller design space.

As a case study for the plant and controller co-optimization an active vibration isolation system with a power-constrained H_2-optimal static state feedback controller is considered. The simultaneous optimization problem shows to be sensitive to numerical instability which limits the convergence of the plant and controller co-optimization algorithm. Input and output normalization, a balanced realization and pole placement are used for numerical conditioning of the optimization problem. For the pole placement, convexified matrix inequalities are developed that confine the closed-loop system poles to a disc centered around the origin and to the plane left of a vertical line. The case study shows that improved closed-loop systems can be obtained with the iterative co-optimization approach, but numerical instability requires termination of the iterative algorithm before an optimum is reached with the plant and controller co-optimization.

Contents

1 Introduction

The theory and methods that are used in the subsequent paper are not part of the standard curriculum of the master Systems and Control. Therefore, the goal of this section is to provide a brief introduction to the theory and methods to help the reader understand the paper. The introduction begins with a short overview on active vibration isolation systems which will be the subject of plant and controller co-optimization. Then, a brief introduction to Linear Matrix Inequalities (LMIs) is provided. LMIs are interesting since many control problems can be cast as an LMI problem and LMIs can be solved relatively efficient for which a large number of open source solvers are available. Some properties of LMIs and operations such as congruence transforms and the Schur complement will be treated here since these are essential tools for LMI problems. Furthermore, the topic of pole placement through LMI regions is introduced. In the appendix, observations will be treated that are unfinished results but may be relevant for further research on the topic.

1.1 Active vibration isolation systems

The performance of high-precision equipment is limited by the disturbances that act on the system. Typically, vibration isolation systems are used to limit the effects of these disturbances. Vibration isolation systems can either be passive or active. An Active Vibration Isolation System (AVIS) contains one or more actuators and uses controllers to achieve or improve the vibration isolation. A typical model for an AVIS with actuation force f_a is shown in Figure 1. Mass m_1 can be interpreted as the mounting platform and mass m_2 represents an internal frame of the machine. Stiffness and damping k_1 and d_1 correspond to the stiffness and damping of the mount and stiffness k_2 and d_2 correspond to the internal stiffness and damping of the precision machinery. The objective of a vibration isolation system is to minimize the deformation of the high precision equipment or, in other words, minimize $x_2 - x_1$. This internal deformation is of interest since in this frame, payloads are handled or samples are scanned by the precision machinery.

Disturbances that are taken into account are floor accelerations $\ddot{x}_0$ and direct disturbances F_d. Examples of a direct disturbance force are a reaction forces due to handling a payload or turbulence in cooling channels.

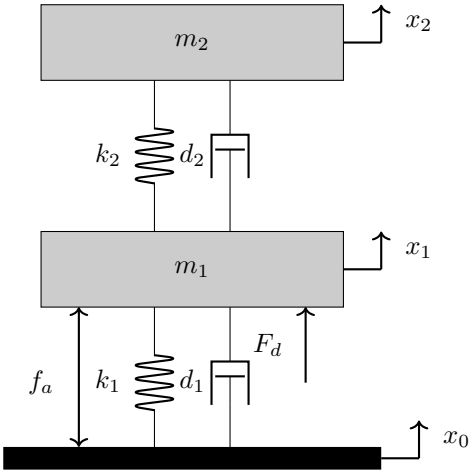

Figure 1: Ideal physical model of an AVIS

For a passive vibration isolation system, the design of the vibration isolation system is often a trade-off between a 'hard' and 'soft' mount. A hard mount has relatively high stiffness k_1 and damping d_1 and a soft mount is more compliant and has less damping. This trade-off can be visualized with transfer functions

$$C(s) = \frac{X_1(s)}{F_d(s)},\ T(s) = \frac{s^2 X_1(s)}{s^2 X_0(s)},\ D(s) = \frac{\Delta X(s)}{F_d(s)},\ T_d(s) = \frac{\Delta X(s)}{s^2 X_0(s)}, \tag{1}$$

where $C(s)$ is called the compliance, $T(s)$ the transmissibility, $D(s)$ the deformability and $T_d(s)$ the deformation transmissibility.

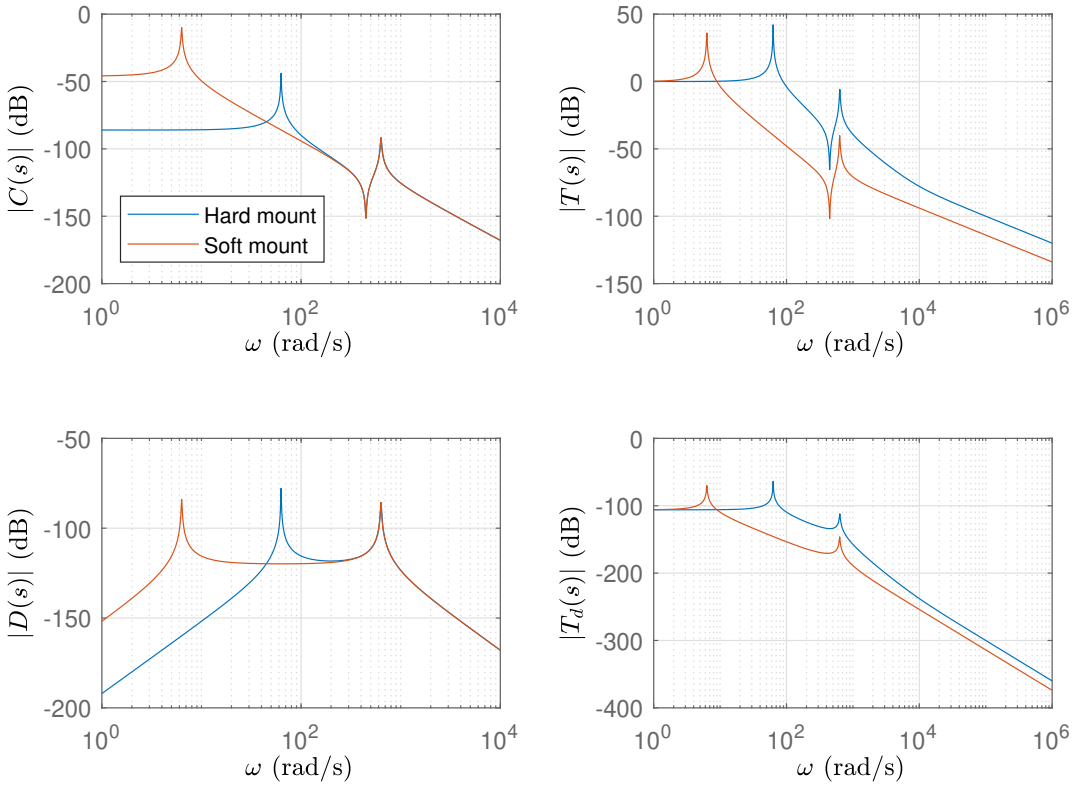

Figure 2: Bode magnitude plots showing the compliance, transmissibility, deformability and deformation transmissibility for a hard and soft mount.

Along the lines of an example of Van der Poel (2010), bode plots of the transfer function for a hard and soft mount vibration isolation system are plotted in Figure 2. This figure shows that a hard mount provides low-frequency attenuation for the compliance and deformability whereas a soft mount provides attenuation on the high-frequency range for the transmissibility and the deformation transmissibility. This trade-off can be summarized as that the hard mount provides attenuation for the low-frequency spectrum of the direct disturbances and a soft mount provides isolation from floor accelerations in the high-frequency range.

1.2 Linear Matrix Inequalities

This section provides an overview of LMIs and is an adaptation from Scherer and Weiland (2011). For more information, the reader is referred to the comprehensible treatments of the topic by Dettori (2001) and Skelton (2021).

A linear matrix inequality is an inequality of the form

$$F(x) = F_0 + F_1 x_1 + F_2 x_2 + \cdots + F_n x_n \succ 0, \tag{2}$$

where F_i are Hermitian matrices, i.e. $F_i = \overline{F_i}^T$ meaning that matrix F_i equals its complex conjugated transpose. The vector $x = (x_1, \ldots, x_n)$ is a vector of real numbers which elements are used as decision variables. The vector x can also be extended to matrix valued decision variables, as is often the case for control applications.

Solving an LMI can be treated as a feasibility problem, i.e. does a vector x exist such that the LMI is satisfied? Alternatively, LMIs can be used for optimization problems. Given an objective, dependent on x, which set of x minimizes or maximizes the objective function while satisfying the LMIs?

An important aspect in optimization is convexity. A function $F(x)$ is convex if for all x_1, x_2 and $\alpha \in (0, 1)$ it holds that

$$F(\alpha x_1 + (1-\alpha)x_2) \preceq \alpha F(x_1) + (1-\alpha)F(x_2). \tag{3}$$

If, $F(x)$ is convex and a stationary point x_s is found, then $F(x_s)$ is the minimal value of $F(x)$. Furthermore, if a function $F(x)$ has strong convexity, i.e. a strict inequality is used for (3), then if a stationary point x_s is found for $F(x)$, this stationary point is the only stationary point and $F(x_s)$ is the global minimum of $F(x)$. Similarly, a function $F(x)$ is concave if

$$F(\alpha x_1 + (1-\alpha)x_2) \succeq \alpha F(x_1) + (1-\alpha)F(x_2). \tag{4}$$

For a concave function, if a stationary point x_s is found, then $F(x_s)$ is a maximum. Note that the term convexity is somewhat loosely used to indicate either that a function is convex or concave. Since LMIs are affine in its decision variables, the feasible region is a polyhedron, which is a convex region. Therefore, any LMI is convex, and if a feasibility or optimization problem can be cast in an LMI, then convexity is guaranteed for this problem.

We can also consider a system of LMIs,

$$F_1(x) \succ 0, F_2(x) \succ 0, \ldots, F_n(s) \succ 0. \tag{5}$$

A system of LMIs can be written as a single LMI following

$$F(x) = \begin{bmatrix} F_1(x) & 0 & \cdots & 0 \\ 0 & F_2(x) & & 0 \\ \vdots & & \ddots & \vdots \\ 0 & 0 & \cdots & F_n(x) \end{bmatrix}. \tag{6}$$

Furthermore, affine constraints can be incorporated in an LMI problem, such as for example

$$\begin{cases} F(x) \succ 0, \\ Ax = b, \end{cases} \tag{7}$$

for some given matrix A and vector b.

For scalars, examining inequalities is trivial. For matrices, with a matrix inequality $F \succ 0$ we mean that $x^T F x > 0$ for any non-zero x. We therefore have $F \succ 0$ if and only if all eigenvalues of F are greater than zero. Note that any matrix can be rewritten as a sum of its symmetric and skew-symmetric parts. Thus, $F = F_{sym} + F_{skew}$ with $F_{sym} = \frac{1}{2}(F + F^T)$ and $F_{skew} = \frac{1}{2}(F - F^T)$. Skew-symmetric matrices have the property that any eigenvalue is either zero or purely imaginary. Hence, $x^T F_{skew} x = 0$ for any x. Therefore, without loss of generality, we can say that if we consider an LMI $F \succ 0$, then F can be assumed to be symmetric (Skelton (2021)).

As stated before, LMIs are useful for many control or stability problems. A well known LMI feasibility problem is Lyapunov's stability requirement. For a system $\dot{x} = Ax$, asymptotic stability is guaranteed if a matrix $P = P^T \succ 0$ can be found such that $A^T P + PA \prec 0$. Typical LMI optimization problems in control encompass the calculation of system norms such as the H_2 and H_∞ norms. If the controller gains for a closed loop system are considered as decision variables, then the optimization problem can yield the optimal closed loop system norm as well as the optimal controller.

1.3 Congruence transforms

As described, solving an LMI comes down to determining the definiteness of the eigenvalues of an LMI. There exist a transform, called a congruence transform, that does not affect the sign of the eigenvalues. For example, if we have a matrix F satisfying $F \succ 0$ then for any non-singular T we have $T^H F T \succ 0$, where T^H is the Hermitian transpose of T.

1.4 Schur complement

Consider a partitioned LMI

$$F = \begin{bmatrix} F_{11} & F_{12} \\ F_{21} & F_{22} \end{bmatrix} \succ 0, \tag{8}$$

with $F_{12} = F_{21}^T$. By application of a congruence transform with

$$T = \begin{bmatrix} I & 0 \\ -F_{22}^{-1} F_{21} & I \end{bmatrix}, \tag{9}$$

the LMI is diagonalized and we find

$$T^H F T = \begin{bmatrix} F_{11} - F_{12} F_{22}^{-1} F_{21} & 0 \\ 0 & F_{22} \end{bmatrix} \succ 0. \tag{10}$$

Simarly, by application of a congruence transform with

$$T = \begin{bmatrix} I & -F_{11}^{-1} F_{12} \\ 0 & I \end{bmatrix}, \tag{11}$$

we find

$$T^H F T = \begin{bmatrix} F_{11} & 0 \\ 0 & F_{22} - F_{21} F_{11}^{-1} F_{12} \end{bmatrix} \succ 0. \tag{12}$$

Since the LMIs above are diagonalized, we can conclude that $F \succ 0$, if and only if

$$\begin{cases} F_{11} - F_{12} F_{22}^{-1} F_{21} \succ 0, \\ F_{22} \succ 0, \end{cases} \tag{13}$$

if and only if

$$\begin{cases} F_{11} \succ 0, \\ F_{22} - F_{21} F_{11}^{-1} F_{12} \succ 0. \end{cases} \tag{14}$$

This result is called the Schur complement. The Schur complement provides a tool for transforming inequalities with rational functions into an LMI. Note that the Schur complement works two ways, if (13) and (14) hold, then neccesarily (8) also holds.

1.5 LMI regions

There are reasons to allow system poles only to specific regions of the complex plane. For example, system stability is guaranteed if all system poles lie in the left-half complex plane for a continuous time system and within the unit circle for discrete time systems. Also other regions can be thought of to, for example, add extra robustness or limit a system's bandwidth.

This pole placement can be achieved using LMI regions. Each region specification yields an LMI that, if satisfied, guarantees that the system poles lie in the respective region. An intersection of LMI regions can easily be formed by satisfying all LMIs that form the intersection.

The following is an adaptation of Scherer and Weiland (2011), showing how LMIs region formulations are developed. Furthermore, LMIs for the stability regions of a continuous time and discrete time system are developed as examples.

Consider a pole $s \in \mathbb{C}$ with complex conjugate $\overline{s}$ and suppose we want this pole to lie in the region described by $Q + sS + \overline{s}S^T + \overline{s}Rs \prec 0$ for some real-valued matrices Q, S and R. The eigenvalues of a real-valued matrix A are contained in this region if we can find a $P \succ 0$ such that

$$\begin{bmatrix} I \\ A \otimes I \end{bmatrix}^T \begin{bmatrix} P \otimes Q & P \otimes S \\ P \otimes S^T & P \otimes R \end{bmatrix} \begin{bmatrix} I \\ A \otimes I \end{bmatrix} \prec 0, \tag{15}$$

where $\otimes$ is the Kronecker product, defined as

$$A \otimes B = \begin{bmatrix} A_{11}B & \dots & A_{1n}B \\ \vdots & & \vdots \\ A_{m1}B & \dots & A_{mn}B \end{bmatrix}. \tag{16}$$

For stability of continuous time system $\dot{x} = Ax$, we require that all eigenvalues of a system matrix A lie in the left-half complex plane, or $Re(s) < 0$, which is equivalent to $s + s^T < 0$. Thus, we can define the LMI region with $Q = 0$, $S = S^T = 1$ and $R = 0$, or

$$\begin{bmatrix} I \\ A \end{bmatrix}^T \begin{bmatrix} 0 & P \\ P & 0 \end{bmatrix} \begin{bmatrix} I \\ A \end{bmatrix} \prec 0. \tag{17}$$

Working out the matrix products yields the well known inequality $A^TP + PA \prec 0$. Thus, all eigenvalues of system matrix A lie in the left-half complex plane if we can find a $P \succ 0$ such that $A^TP + PA \prec 0$.

Another important LMI region is the unit circle around the origin as this is the stability region for the discrete time domain. A unit circle can be described as $|s| < 1$, or $\overline{s}s < 1$ or $\overline{s}s - 1 < 0$. Note that this region is described with $R = 1$ and $Q = -1$. So, we have

$$\begin{bmatrix} I \\ A \end{bmatrix}^T \begin{bmatrix} -P & 0 \\ 0 & P \end{bmatrix} \begin{bmatrix} I \\ P \end{bmatrix} \prec 0, \tag{18}$$

which can be rewritten as $-P + A^TPA \prec 0$. Thus, the eigenvalues of A lie within the unit circle if we can find a $P \succ 0$ such that $-P + A^TPA \prec 0$.

Plant and Controller Co-optimization for an Active Vibration Isolation System Using Convexified LMIs

G.H.W. Schrijver *

* *University of Twente, Faculty of Electrical Engineering, Mathematics and Computer Science, PO 217, 7500AE Enschede, The Netherlands (e-mail: g.h.w.schrijver@student.utwente.nl).*

Abstract: Simultaneous optimization of a plant and controller is generally a nonlinear problem. Several works have studied this problem, often resulting in an iterative approach. This paper investigates the plant and controller co-optimization for an active vibration isolation system and a power-constrained H_2-optimal static state feedback controller by iterative use of convexified LMI formulations. Pole placement is considered through LMI regions and convexified LMI formulations are developed for pole placement within an origin-centered disc and the plane to the left of a vertical line. The simultaneous optimization problem shows to be sensitive to numerical instability. Input and output normalization, a balanced realization and pole placement are proposed for numerical conditioning of the optimization problem. A case study shows that improved closed-loop systems can be found but the numerical instability requires termination of the iterative algorithm before a stationary point in the co-optimization is found.

Keywords: Hardware/software co-design, Vibration control, Parametric optimization, Convex optimization, Stochastic optimal control problems, Descriptor systems, Constrained control

1. INTRODUCTION

The common methodology for system design is to determine specifications for the plant and the controller and optimize them independently. Although the plant and controller may be optimal for their respective design specifications, the independent design may lead to a sub-optimal design for the closed loop system (Fathy et al. (2001)).

For an optimal closed loop performance, the plant and controller need to be co-optimized (Kajiwara and Nagamatsu (1999), Roos (2007)). In general, the co-optimization of the plant and controller is a nonlinear problem which can be approached with different strategies. Veen et al. (2014) use a gradient based strategy in the frequency domain where the sensitivity function is minimized for a particular set of frequencies. This concept is extended for a MIMO system and with additional mechanical requirements in Van der Veen et al. (2017). Kianfar and Fredriksson (2011) propose the vertex enumeration method. The claim here is that if the plant parameters belong to a polytope, the optimal plant and controller combination can be found at a vertex of this polytope. This method then reduces the plant and controller co-optimization problem to calculating an optimal controller at a finite number of vertices and selecting the vertex with the optimal plant and controller performance. The usefulness of this method is limited as will be indicated with an example in this paper. Hiramoto and Grigoriadis (2006) solve a system and mixed H_2/H_∞ controller co-design by iteratively solving LMIs that are a linear approximation to the co-optimization problem. First order terms that appear nonlinearly in products are neglected with the argument that these will be small terms. Shimomura and Fujii (2000) propose the successive over-bounding method for multi-objective controller design. With this method, matrix inequalities are linearized by replacing nonlinear terms with suitable quadratic upper bounds. This method is equivalent but has emerged independently from the use of so-called convexifying potentials in Oliveira et al. (2000), which uses the addition of suitable semi-definite terms to nonlinear terms in matrix inequalities. If these semi-definite terms are chosen following a specific structure, the addition of this term linearizes or 'convexifies' the matrix inequalities. Due to the semi-definiteness of the added term, a solution of the convexified problem will necessarily also be a solution to the original problem. The use of convexifying potentials and the use of the successive over-bounding technique on plant and controller co-optimization have been demonstrated on two problems that are very similar to each other in Camino et al. (2003) and Kim et al. (2005). The use of convexifying potentials for plant and controller co-optimization is extended by Goyal and Skelton (2019) by taking sensor and actuator precision into account such that a hardware price for a system can be added to the optimization. The same strategy is applied is used in Goyal et al. (2021) and Chen et al. (2023) with application to tensegrity systems.

Plant and controller co-optimization is particularly interesting for applications that require effective attenuation of disturbances such as wafer scanners (Heertjes et al. (2020)), sensitive optical equipment such as gravitational wave detectors (Matichard et al. (2015)) and scanning electron microscopes (Shin et al. (2020)). Often, high-precision machinery is mounted on a vibration isolation system. If this mount is also actuated, we are speaking of

an active vibration isolation system (AVIS) (Van der Poel (2010)). AVIS are often designed such that the deformation of an internal mode of the high-precision machinery is minimized.

Plant and controller co-optimization for AVIS systems has been investigated by Spanjer and Hakvoort (2022) using a combination of Ricatti equality-based H_2 controller synthesis and a grid search over plant parameters. In this work it was found that using a Ricatti equality-based synthesis provides insufficient flexibility in combining different types of system norms, in particular H_∞ norms for robustness guarantees. H_∞ norms have been approximated by H_2 norms which introduces a considerable conservatism to the optimization. Switching to an LMI-based optimization provides the flexibility to combine different norms and reduce conservatism in the optimization. Furthermore, the number of system parameters for the optimization is limited for a grid search strategy as the computational complexity increases exponentially with the number of optimization parameters.

In this paper, the plant parameters and a static full state H_2 will be co-optimized for an AVIS. To accomplish this, a strategy similar to Camino et al. (2003) will be used since this paper demonstrates a plant and controller co-optimization for a system similar to an AVIS and it uses LMI formulations for the co-optimization. The objective will be to design an AVIS such that the covariance of the internal deformation is minimized given a limited actuation power. Beside the plant and controller co-optimization for an AVIS, other contributions of this paper are a treatment of numerical conditioning methods for solving convexified plant and controller co-optimization problems. Furthermore, this paper provides convexified formulations for some LMI regions and proposes pole placement as a tool for improving numerical accuracy.

This paper is organized as follows. Section 2 commences with a descriptor state space formulation for a plant with affine dependence on its parameters. Then, LMI formulations are developed for H_2 static state feedback, convexified plant and H_2 static state feedback co-optimization and convexified LMI regions for plant and controller co-optimization. Furthermore, an algorithm is proposed that iteratively searches for an optimal plant and controller and adheres to pole placement restrictions. In section 3 the co-optimization algorithm will be applied to an AVIS system. A model is developed for an AVIS and numerical conditioning is discussed. Sections 4, 5 and 6 respectively provide the results of, a discussion on and a conclusion of the co-optimization for the AVIS system. Appendix A contains a discussion on how power constraint can be applied in the presence of multiple actuators and Appendix B provides an example for which the vertex enumeration method will not find the optimal solution.

In this paper, $\mathbb{E}[.]$ is the expectation oparator and Tr is the trace operator. Inequality operators $<$ and $>$ are used for scalar inequalities and $\prec$ and $\succ$ are used for matrix inequalities. Furthermore, for short notation, $(.)^{-T}$ is used for $((.)^T)^{-1}$.

2. PLANT AND CONTROLLER CO-OPTIMIZATION

In this chapter, a general parameter-dependent plant model is posed in descriptor state space formulation. Using this model formulation, LMI formulations are developed to calculate an H_2 state feedback controller for a constant system as well as convexified LMI formulations for finding an H_2-optimal plant and controller. LMIs will be provided for pole placement in case of optimization for a constant plant and convexified formulations will be derived for plant and controller co-optimization. For the pole placement, guaranteed damping and an origin-centered disc are considered. At last, an algorithm is given to iteratively find an H_2-optimal plant and controller.

2.1 Descriptor state space formulation

Consider a linear dynamical plant with affine dependence on its parameters. Suppose that these parameters depend on weighting factor α, the dynamics of the plant can be described as

$$E(\alpha)\dot{x} = A(\alpha)x + B_w(\alpha)w + B_u u, \tag{1a}$$
$$z = C_z x, \tag{1b}$$

with state vector x, disturbance vector w, input vector u and output vector z. This formulation is also known as a descriptor state space formulation. This formulation differs from the standard state space formulation by matrix $E(\alpha)$ which typically contains the masses and moments of inertia for mechanical systems and inductances for electrical systems. The descriptor state space formulation is adopted to avoid multiplication with the inverse inertias or inductances and thus keeping an affine dependence in these parameters. The dependence of the matrices on the plant parameters can be expressed as

$$\begin{aligned} E(\alpha) &= E_0 + \sum_i \alpha_i E_i, \\ A(\alpha) &= A_0 + \sum_i \alpha_i A_i, \\ B_w(\alpha) &= B_{w,0} + \sum_i \alpha_i B_{w,i}, \end{aligned} \tag{2}$$

where $(E(\alpha), A(\alpha), B_w(\alpha)) = (E_0, A_0, B_{w,0})$ constitutes the nominal plant model. E_i, A_i and $B_{w,0}$ contain the terms of the system matrices that depend on plant parameter i and are added with weighting factor a_i to obtain the parameter dependent plant dynamics. Effectively, this formulation describes plant parameter p_i as

$$p_i = (1 + \alpha_i)p_{i,0}, \tag{3}$$

where $p_{i,0}$ is the nominal value for parameter p_i and α_i its respective weight.

Note that only systems with a constant B_u are considered since these systems have an affine dependence on input u.

2.2 H_2-optimal static state feedback synthesis

In this paper, a stochastic approach is used. Disturbance signals are assumed white and zero-mean stochastic signals and the objective is to minimize the asymptotic variance of an output signal. The equivalence of a covariance controller

to an H_2 optimization problem is shown in (Skelton et al. (2017), Dettori (2001)). For the controller we will use static state feedback, using feedback law

$$u(t) = Kx(t), \tag{4}$$

yielding the closed loop system matrix

$$A_{cl} = A + B_u K. \tag{5}$$

Theorem 1 and 3 are adapted from Camino et al. (2003). Instead of optimizing the control signal with output constraints we will optimize the output with a constraint on the power of the control signal.

Theorem 1. Considering a zero-mean white noise signal $w(t)$ with asymptotic covariance matrix $\lim_{t\to\infty} \mathbb{E}[w(t)w(t)^T] = W \succ 0$. Let the asymptotic variance of a 1-dimensional control signal be bounded by ζ, i.e. $\lim_{t\to\infty} \mathbb{E}[u(t)^T u(t)] < \zeta$. Then, the H_2 norm of a closed loop system with constant plant parameters $H_{zw}(s) := C_z(sI - E^{-1}A_{cl})^{-1}E^{-1}B_w$ is bounded by $\sqrt{\gamma}$, i.e. $||H_{zw}(s)||_2 < \sqrt{\gamma}$ if for a $P = P^T \succ 0$ a feasible solution can be found to

$$\begin{bmatrix} * & B_w \\ B_w^T & -W^{-1} \end{bmatrix} \prec 0, \tag{6a}$$

$$\begin{bmatrix} \zeta & F \\ F^T & P \end{bmatrix} \succ 0, \tag{6b}$$

$$C_z P C_z^T \prec Z, \tag{6c}$$

$$\mathrm{Tr}(Z) < \gamma, \tag{6d}$$

where $* = APE^T + EPA^T + B_uFE^T + EF^TB_u^T$. The feedback gain matrix K is obtained by $K = FP^{-1}$.

Proof. The H_2-norm of a closed loop system in regular state space formulation $H_{zw}(s) := C_z(sI - \hat{A}_{cl})^{-1}\hat{B}_w$ is bounded by $\sqrt{\gamma}$ if for a $P = P^T \succ 0$ a feasible solution can be found to (see for example Dettori (2001), Skelton et al. (2017), Scherer and Weiland (2011), Caverly and Forbes (2021))

$$\hat{A}_{cl}P + P\hat{A}_{cl}^T + \hat{B}_w W \hat{B}_w^T \prec 0, \tag{7a}$$

$$C_z P C_z^T \prec Z, \tag{7b}$$

$$\mathrm{Tr}(Z) < 0. \tag{7c}$$

When considering a system that in its descriptor representation, i.e. $H_{zw}(s) := C_z(sI - E^{-1}A_{cl})^{-1}E^{-1}B_w$, we have $\hat{A}_{cl} = E^{-1}A_{cl}$ and $\hat{B}_w = E^{-1}B_w$. Then, (7a) takes the form $E^{-1}A_{cl}P + PA_{cl}^TE^{-T} + E^{-1}B_wWB_w^TE^{-T} \prec 0$. Applying a congruence transform with E^{-1} yields

$$A_{cl}PE^T + EPA_{cl}^T + B_wWB_w^T \prec 0. \tag{8}$$

When considering static full state feedback, we have $A_{cl} = A + B_uK$, which causes a nonlinearity in variables K and P. A linear inequality can be obtained with the substitution $(P, KP) \to (P, F)$. Applying a Schur complement to (8) and applying the substitution, (7a) becomes

$$\begin{bmatrix} APE^T + EPA^T + B_uFE^T + EF^TB_u^T & B_w \\ B_w^T & -W^{-1} \end{bmatrix} \prec 0.$$

The asymptotic variance of the control signal is a measure of the average controller power (Boyd and Barratt (1991)). The asymptotic variance of the control signal is given as

$$\begin{aligned} \lim_{t\to\infty} \mathbb{E}[u(t)^T u(t)] &= \lim_{t\to\infty} \mathrm{Tr}(\mathbb{E}[u(t)u(t)^T]) \\ &= \lim_{t\to\infty} \mathrm{Tr}(\mathbb{E}[Kx(t)x(t)^T K^T]) \\ &= \mathrm{Tr}(KP_0K^T) \\ &\leq \mathrm{Tr}(KPK^T) \end{aligned} \tag{9}$$

where P_0 is the asymptotic covariance matrix of the system states, i.e. $P_0 = \lim_{t\to\infty} \mathbb{E}[x(t)x(t)^T]$ (Skelton et al. (2017), Dettori (2001)). When considering a single controller output, i.e. a single actuator, the upper bound on the asymptotic variance of the control signal reduces to $\lim_{t\to\infty} \mathbb{E}[u(t)^T u(t)] \leq KPK^T$. Using the coordinate transform, this relation becomes $\lim_{t\to\infty} \mathbb{E}[u(t)^T u(t)] \leq FP^{-1}F^T$. Bounding the asymptotic variance by ζ and applying a Schur complement yields

$$\begin{bmatrix} \zeta & F \\ F^T & P \end{bmatrix} \succ 0. \tag{10}$$

Remark 2. Note that this holds if only one actuator is considered. In case there are multiple actuators, different formulations are possible for the controller power constraints (see Appendix A).

□

2.3 Plant and controller co-optimization

For simultaneous optimization of the plant and controller, the plant parameters will be treated as optimization parameters. Therefore, the system matrices $E(\alpha)$, $A(\alpha)$ and $B_w(\alpha)$ explicitly depend on the plant parameter weighting factors α. Inequality 6a in Theorem 1 then becomes

$$\begin{bmatrix} * & B_w(\alpha) \\ B_w(\alpha)^T & -W^{-1} \end{bmatrix} \prec 0, \tag{11}$$

with $* = A(\alpha)PE(\alpha)^T + E(\alpha)PA(\alpha)^T + B_uFE(\alpha)^T + E(\alpha)F^TB_u^T$, or $* = (A(\alpha)+B_uK)PE(\alpha)^T + E(\alpha)P(A(\alpha)+B_uK)^T$ without the variable substitution. Using the plant parameters in the optimization renders the problem nonlinear and non-convex. Camino et al. (2003) has shown how to locally convexify a similar problem by noting that a potential function can be used to linearize the problem (see Oliveira et al. (2000)).

Theorem 3. Considering a matrix $G = (A_c+B_uK_c-E_c)P_c$ for some constant matrices A_c, K_c, E_c and P_c. The H_2 norm of a static state feedback closed loop system

$$H_{zw}(s, \alpha) := C_z(sI - E(\alpha)^{-1}A_{cl}(\alpha))^{-1}E(\alpha)^{-1}B_w(\alpha),$$

under the assumption of a white noise zero-mean disturbance $w(t)$ and a limited asymptotic variance of the controller signal, i.e. $\lim_{t\to\infty} \mathbb{E}[u(t)^T u(t)] < \zeta$, is bounded by $\sqrt{\gamma}$ if there exist a set of plant parameters weights α, a feedback gain matrix K and a matrix $Q = Q^T \succ 0$ such that the following LMIs are satisfied:

$$\begin{bmatrix} * & B_w(\alpha) & A(\alpha)+B_uK & E(\alpha) \\ B_w(\alpha)^T & -W^{-1} & 0 & 0 \\ A(\alpha)^T+K^TB_u^T & 0 & -Q & 0 \\ E(\alpha)^T & 0 & 0 & -Q \end{bmatrix} \prec 0, \tag{12a}$$

$$\begin{bmatrix} \zeta & K \\ K^T & Q \end{bmatrix} \succ 0, \tag{12b}$$

$$\begin{bmatrix} Z & C_z \\ C_z^T & Q \end{bmatrix} \succ 0, \tag{12c}$$

$$\mathrm{Tr}(Z) < \gamma, \tag{12d}$$

where

$$* = -(A(\alpha)+B_uK-E(\alpha))G^T$$
$$-G(A(\alpha)+B_uK-E(\alpha))^T+GQG^T.$$

Proof. Notice that the nonlinearity of the problem appears in the term (dropping the dependence on α for short notation and using $A_{cl}=A+B_uK$)

$$A_{cl}PE^T+EPA_{cl}^T.$$

By completion of squares, this term can be rewritten as

$$A_{cl}PA_{cl}^T+EPE^T-(A_{cl}-E)P(A_{cl}-E)^T.$$

By applying a Schur complement on the terms $A_{cl}PA_{cl}$ and EPE^T, (11) can be written as

$$\begin{bmatrix} -(A_{cl}-E)P(A_{cl}-E)^T & B_w & A_{cl} & E \\ B_w^T & -W^{-1} & 0 & 0 \\ A_{cl}^T & 0 & -P^{-1} & 0 \\ E^T & 0 & 0 & -P^{-1} \end{bmatrix} \prec 0. \tag{13}$$

The term in the top left corner of this formulation still contains multiplications between optimization variables. Furthermore, both P and its inverse appear in this matrix inequality.

Let $A_{cl,c} := A_c + B_uK_c$, E_c and P_c be some constant matrices and define a function

$$\Phi = (A_{cl}-E-GP^{-1})P(A_{cl}-E-GP^{-1})^T,$$

with $G=(A_{cl,c}-E_c)P_c$. Notice that, since P is positive definite, it follows that Φ is positive semi-definite. If we were to add Φ to the top-left block of (13) and find a feasible solution to the resulting LMI, then due to the positive semi-definiteness of Φ, this solution is guaranteed to also satisfy (13). Adding the potential to the term in the top-left corner yields

$$-(A_{cl}-E)P(A_{cl}-E)^T+\Phi =$$
$$-(A_{cl}-E)G_c^T-G_c(A_{cl}-E)^T+GP^{-1}G_c^T$$

which is linear in E, $A_{cl}=A+B_uK$ and P^{-1}. With applying the transformation $P^{-1}\rightarrow Q$ we arrive at (12a). Note that if $A_{cl,c}$, E_c and P_c are chosen as a feasible solution for (6), then Φ vanishes for $(A_{cl},E,P)=(A_{cl,c},E_c,P_c)$ and the formulations of (11) and (12a) become equivalent.

The same transformation has to be applied to the inequality $C_zPC_z^T = C_zQ^{-1}C_z^T \prec Z$. With a Schur complement,this inequality can be rewritten to

$$\begin{bmatrix} Z & C_z \\ C_z^T & Q \end{bmatrix} \succ 0.$$

The same applies for the power limitation on the controller signal $KPK^T=KQ^{-1}K^T<\zeta$, which by using a Schur complement becomes

$$\begin{bmatrix} \zeta & K \\ K^T & Q \end{bmatrix} \succ 0.$$

□

2.4 LMI regions

With the use of LMI regions, the pole locations of a closed loop system can be restricted to specified regions on the complex plane. This can be accomplished by extending the optimization problem with extra LMIs. Several LMI formulations for regions on the complex plane have been developed and for an overview, the reader is referred to Scherer and Weiland (2011). When the plant parameters are used as optimization variables, the inequalities describing the LMI regions usually become nonlinear. In order to combine plant and controller co-optimization with LMI regions, convex approximations of the respective LMI regions have to be made. Furthermore, the LMI region formulations need to be compatible with the coordinate systems used in (6) and (12).

Not all LMI regions are suitable for convexification since only nonlinear terms on the diagonal of the matrix inequalities can be linearized. Typically, regions that have non-orthogonal borders such as a conic sector lead to off-diagonal nonlinearities.

In this paper two types of LMI regions are considered, namely guaranteed damping and a disc centered at the origin.

Theorem 4 and 6 describe the LMI regions for a system with constant parameters. These formulations are considered general results. Theorem 5 and 7 are novel formulations, describing convexified formulations for parameter-dependent systems.

Guaranteed damping Let β be a positive real number. The LMI region corresponding to a guaranteed damping can be described as

$$\{s\in\mathbb{C}|Re(s)<-\beta\}.$$

Theorem 4. The poles of a feasible closed loop system with constant parameters in (6) are in the region $\{s\in\mathbb{C}|Re(s)<-\beta\}$ by extending (6) with the LMI

$$2\beta EPE^T+APE^T+EPA^T+B_uFE^T+EF^TB_u^T\prec 0. \tag{14}$$

Proof. The LMI region for guaranteed damping with the standard state space formulation is given as (Scherer and Weiland (2011))

$$2\beta Q+Q\hat{A}_{cl}+\hat{A}_{cl}^TQ\prec 0. \tag{15}$$

To be compatible with (6), we require the use of its dual version, i.e. use $P=Q^{-1}$. Applying a congruence transform with P and adopting the descriptor state space formulation for the closed loop system (i.e. $\hat{A}_{cl}=E^{-1}A_{cl}$), then (15) can be rewritten as

$$2\beta EPE^T+(A+B_uK)PE^T+EP(A+B_uK)^T\prec 0. \tag{16}$$

And using the substitution $(P, KP) \rightarrow (P, F)$ the result is

$$2\beta EPE^T + APE^T + EPA^T + B_uFE^T + EF^TB_u^T \prec 0. \quad (17)$$

□

Theorem 5. For some $G = (A_c + B_uK_c - E_c)P_c$ with constant matrices A_c, K_c, E_c and P_c, the poles of a feasible closed loop system for (12) are in the region $\{s \in \mathbb{C} | Re(s) < -\beta\}$ by extending (12) with the LMI

$$\begin{bmatrix} * & A(\alpha) + B_uK & E(\alpha) \\ (A(\alpha) + B_uK)^T & -Q & 0 \\ E(\alpha)^T & 0 & -\frac{Q}{1+2\beta} \end{bmatrix} \prec 0, \quad (18)$$

where

$$* = -(A(\alpha) + B_uK - E(\alpha))G^T$$
$$-G(A(\alpha) + B_uK - E(\alpha))^T + GQG^T.$$

Proof. The steps taken are identical to the proof of Theorem 3, except that the term $(1 + 2\beta)EPE^T$ is used for a Schur complement instead of the term EPE^T.

□

Disc centered at the origin Considering a disc with radius r, centered at the origin. The region of this disc can be described as

$$\{s \in \mathbb{C} | \, |s| < r\}.$$

Theorem 6. The poles of a feasible closed loop system with constant parameters in (6) are in the region $\{s \in \mathbb{C} || s| < r\}$ by extending (6) with the LMI

$$\begin{bmatrix} -r^2P & (AP + B_uF)^T \\ AP + B_uF & -EPE^T \end{bmatrix} \prec 0. \quad (19)$$

Proof. The LMI region for the inside of a circle centered at the origin with radius r is given by (see Scherer and Weiland (2011))

$$-r^2Q + \hat{A}_{cl}^T Q \hat{A}_{cl} \prec 0. \quad (20)$$

We require the dual version of this formulation for compatibility with the coordinates used in (6), i.e. $P = Q^{-1}$. Dualizing the above equation and applying a congruence transform with P yields

$$-r^2P + PA^TP^{-1}AP \prec 0.$$

Adopting the descriptor representation, i.e. $\hat{A}_{cl} = E^{-1}A_{cl}$, and writing $A_{cl} = A + B_uK$, we obtain

$$-r^2P + P(A + B_uK)^TE^{-T}P^{-1}E^{-1}(A + B_uK)P \prec 0.$$

The inverse relation in P makes this inequality nonlinear, but this can be resolved by a Schur complement:

$$\begin{bmatrix} -r^2P & P(A + B_uK)^T \\ (A + B_uK)P & -EPE^T \end{bmatrix} \prec 0.$$

Applying the coordinate transform $(P, KP) \rightarrow (P, F)$ yields

$$\begin{bmatrix} -r^2P & (AP + B_uF)^T \\ AP + B_uF & -EPE^T \end{bmatrix} \prec 0. \quad (21)$$

□

Theorem 7. For some matrices E_c and P_c the poles of a feasible closed loop system in (12) are in the region $\{s \in \mathbb{C} || s| < r\}$ by extending (12) with the LMI

$$\begin{bmatrix} -r^2Q & (A(\alpha) + B_uK))^T \\ A(\alpha) + B_uK & * \end{bmatrix} \prec 0, \quad (22)$$

with $* = E_cP_cQP_c^TE_c^T - E_cP_cE(\alpha)^T - E(\alpha)P_c^TE_c^T$.

Proof. Since (12) is in terms of $Q = P^{-1}$, there is no need for dualization of the formulation and we can start with the formulation of the LMI region as

$$-r^2Q + \hat{A}^TQ\hat{A} \prec 0.$$

Adopting the descriptor representation, i.e. $\hat{A}_{cl}$, writing $A_{cl} = A + B_uK$ and considering the dependence on parameter weights α, then the inequality can be Considering the closed loop system, the dependence on α and adopting the descriptor formulation, then the inequality can be written as

$$-r^2Q + (A(\alpha) + B_uK)^TE(\alpha)^{-T}QE(\alpha)^{-1}(A(\alpha) + B_uK) \prec 0.$$

By applying a Schur complement, we can write

$$\begin{bmatrix} -r^2Q & (A(\alpha) + B_uK)^T \\ A(\alpha) + B_uK & -E(\alpha)Q^{-1}E(\alpha)^T \end{bmatrix} \prec 0. \quad (23)$$

A convex approximation of this formulation can be created by adding the positive semi-definite function

$$\Phi = (E_cP_c - E(\alpha)Q^{-1})Q(E_cP_c - E(\alpha)Q^{-1})^T$$

to the right-bottom element, yielding (22).

□

Note that if $A = A_c$, $E = E_c$, $K = K_c$ and $Q^{-1} = P_c$, then (19) and (22) become equivalent. Also, if $Q^{-1} = P_c$ and $E = E_c$, then (14) and (18) become equivalent.

2.5 Iterative co-optimization algorithm

The convex approximations of the the plant and controller co-optimization depend on a particular set of constant matrices which in general cannot be chosen freely. Therefore, first a suitable choice for these matrices has to be determined before the convexified LMI formulations can be used for plant and controller co-optimization. If we chose any feasible solution of (6) or a known solution to (12) and take these constant matrices according this solution, we can always find a solution to (12) since any feasible solution of (6) and (12) is by design always a solution to (12). Then, (12) becomes a convex approximation of the plant and controller co-optimization around the used solution. This attribute of the convexified formulations will be used for an algorithm that iteratively co-optimizes the plant and controller.

Below, an algorithm is described that iteratively optimizes for a closed loop system that has a better performance in terms of objective γ. This algorithm follows closely to the algorithm described in Camino et al. (2003) up to some changes in the LMIs for the optimization objective and the consideration of LMI regions. The algorithm for plant and controller co-optimization is as follows:

Algorithm for plant and controller co-optimization

Initialize nominal plant parameters α_0
Define the LMI regions by setting β and r
Calculate K_0 and P_0 by minimizing γ with the conditions given by (6), (14) and (19)
Set $\gamma_0 \leftarrow \gamma$
Set η to a prescribed tolerance and set $k = 0$
repeat
  Set $(E_c, A_c, P_c, K_c) \leftarrow (E(\alpha_k), A(\alpha_k), P_k, K_k)$
  Set $G \leftarrow (A_c + B_uK_c)P_c$
  Minimize γ subject to (12), (18) and (22) for α, K and Q

Denote the solution $(\alpha^*, K^*, Q^*, \gamma^*)$
Set $(\alpha_{k+1}, K_{k+1}, P_{k+1}, \gamma_k) \leftarrow (\alpha^*, K^*, Q^{*-1}, \gamma^*)$
Set $k \leftarrow k+1$
until $||\gamma_k - \gamma_{k-1}|| < \eta$

Remark 8. The algorithm described above will approach a stationary point that is not necessarily the globally optimal plant and controller pair. Note that a global optimal controller can be found for any α_k by minimization of γ for F and P subject to (6), (14) and (19).

3. CASE STUDY: ACTIVE VIBRATION ISOLATION SYSTEM

3.1 Model

The mechanical part of an AVIS can be modeled as a double mass-spring-damper system with masses m_1 and m_2, stiffnesses k_1 and k_2 and damping constants d_1 and d_2. The system is subject to floor accelerations $\ddot{x}_0$ and a direct disturbance force F_d, which are forces caused by, for example, the handling of a payload or turbulence in cooling channels.

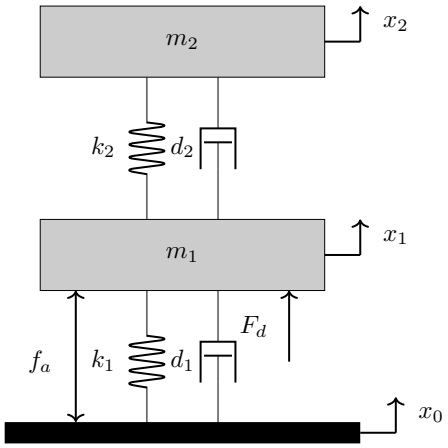

Fig. 1. Ideal physical model of an AVIS.

The system is actuated with actuation force f_a, which is exerted by a motor with motor constant k_m, coil inductance L and coil resistance R. The motor dynamics are modeled as

$$L\dot{f}_a = k_m V - R f_a - k_m^2(\dot{x}_1 - \dot{x}_0), \tag{24}$$

where V is the input voltage.

For simplicity the assumption is made that all states are measurable and without noise. Disturbances that are taken into account are the floor accelerations $\ddot{x}_0$, the direct disturbance force F_d and noise on the input voltage V_d.

A coordinate system that is in terms of relative motions is adopted. We define relative motion to the floor as $\epsilon_1 = x_1 - x_0$ and $\epsilon_2 = x_2 - x_0$. The internal deformation of the AVIS is defined as $\epsilon_3 = x_2 - x_1$.

In descriptor state space formulation, the dynamics of the nominal system is described as:

$$E\dot{x} = Ax + B_w w + B_u u, \tag{25}$$

where

$$E = \begin{bmatrix} 1 & 0 & 0 & 0 & 0 \\ 0 & 1 & 0 & 0 & 0 \\ 0 & 0 & m_1 & 0 & 0 \\ 0 & 0 & 0 & m_2 & 0 \\ 0 & 0 & 0 & 0 & L \end{bmatrix}, B_u = \begin{bmatrix} 0 \\ 0 \\ 0 \\ 0 \\ k_m \end{bmatrix}, B_w = \begin{bmatrix} 0 & 0 & 0 \\ 0 & 0 & 0 \\ -m_1 & 1 & 0 \\ -m_2 & 0 & 0 \\ 0 & 0 & k_m \end{bmatrix},$$

$$A = \begin{bmatrix} 0 & 0 & 1 & 0 & 0 \\ 0 & 0 & 0 & 1 & 0 \\ -k_1 - k_2 & k_2 & -d_1 - d_2 & d_2 & 1 \\ k_2 & -k_2 & d_2 & -d_2 & 0 \\ 0 & 0 & -k_m^2 & 0 & -R \end{bmatrix},$$

$$x = \begin{bmatrix} \epsilon_1 \\ \epsilon_2 \\ \dot{\epsilon}_1 \\ \dot{\epsilon}_2 \\ f_a \end{bmatrix}, u = V, w = \begin{bmatrix} \ddot{x}_0 \\ F_d \\ V_d \end{bmatrix}.$$

3.2 Optimization objective

The objective of the optimization is to minimize the asymptotic variance of the internal deformation of the AVIS system, i.e. minimization of $\lim_{t\to\infty} \mathbb{E}[\epsilon_3(t)^T \epsilon_3(t)]$ by optimizing over plant parameters and static full state feedback controllers while adhering to the actuator power constraint.

With this performance objective the descriptor state space formulation is extended with the output equation

$$z = C_z x, \tag{26}$$

with $C_z = [-1\ 1\ 0\ 0\ 0]$.

3.3 Plant parameters

For this case study, and adaptation of the system in Spanjer and Hakvoort (2022) is used as a basis.

Plant parameter	Value
m_1	5 kg
m_2	2.5 kg
k_1	3.8×10^3 N/m
k_2	2.5×10^5 N/m
d_1	3.4 Ns/m
d_2	2.5 Ns/m
k_m	10 N/A
L	5.2 mH
R	12.8 Ω

Table 1. Nominal plant parameters of the AVIS.

Thermal limits of the actuator induce a limit in the asymptotic variance of the control signal u. Taking the maximum continuous power of the motor $P_{100} = 16$W as a limit, then the asymptotic variance of u is limited by

$$\lim_{t\to\infty} \mathbb{E}[u(t)^T u(t)] = \lim_{t\to\infty} \mathbb{E}[V(t)^T V(t)] \leq R P_{100}. \tag{27}$$

The variances of the disturbances are chosen as $\mathbb{E}[\ddot{x}_0^T \ddot{x}_0] = 10^{-6}[\mathrm{m}^2/\mathrm{s}^4]$, $\mathbb{E}[F_d^T F_d] = 10^{-8}[\mathrm{N}^2]$ and $\mathbb{E}[V_d^T V_d] = 10^{-7}[\mathrm{V}^2]$.

3.4 Numerical conditioning

Since the optimization problems will be solved using floating point operations, we are dealing with limited numerical

precision. Especially, with the iterative algorithm, numerical precision is important since optimization results are used in subsequent optimization steps.

Therefore, strategies are used that condition the numerics of the optimization problem.

Input/Output Scaling In order to reduce the spread in numerical values, the inputs for the optimization problem are normalized such that the variances of the input signals are unitary. The output is rescaled such that the output variance of the optimally controlled nominal system becomes unitary.

For this system, the scaling is as follows. New system matrices $\overline{B_u}$, $\overline{B_w}$, $\overline{C_z}$ and input and output vectors $\overline{u}$, $\overline{w}$ and $\overline{z}$ are calculated such that

$$\begin{aligned} E\dot{x} &= Ax + \overline{B_u}\overline{u} + \overline{B_w}\overline{w}, \\ \overline{z} &= \overline{C_z}x, \end{aligned} \tag{28}$$

with

$$\begin{aligned} \overline{B_u} &= B_u\sqrt{S_u}, \\ \overline{B_w} &= B_w\sqrt{S_w}, \\ \overline{C_z} &= \sqrt{S_z}C_z, \end{aligned} \tag{29}$$

and

$$\begin{aligned} \overline{u} &= S_u^{-1}u, \\ \overline{w} &= S_w^{-1}w, \\ \overline{z} &= S_z^{-1}z, \end{aligned} \tag{30}$$

with

$$S_u = \zeta, S_w = \begin{bmatrix} \mathbb{E}[\ddot{x}_0^T\ddot{x}_0] & 0 & 0 \\ 0 & \mathbb{E}[F_d^T F_d] & 0 \\ 0 & 0 & \mathbb{E}[V_d^T V_d] \end{bmatrix}. \tag{31}$$

And $S_z = \gamma_0$, where γ_0 is the result of minimizing for γ, subject to (6), (14) and (19).

Balanced realization After the rescaling, a balanced realization of the system is calculated. With a balanced realization, the coordinates of the system are transformed such that the controllability and the observability Gramians become equal and diagonal, where the diagonal contains the variances of the states. The effect is that the sensitivity to the inputs and outputs are balanced. For the system matrices the result is that gains are also balanced, which decreases the numerical spreads.

LMI Regions Since Lyapunov matrix P reflect the dynamics of the system, having both slow and fast dynamics in the system can cause a large spread in the eigenvalues of matrix P. Pole placement can be used to bring the pole locations closer and thus lower the condition number of matrix P. We will do this by requiring guaranteed damping and confine the poles to a disc around the origin. From a implementation viewpoint guaranteed damping is also useful to add extra robustness to the stability. The circular disc can be justified as a limited actuator bandwidth. Furthermore, application of the circular disc leads to more robustness to high-frequency parasitic dynamics. Since the pole locations are constrained by LMI regions, the design space is also limited. Therefore, the theoretical performance of the closed-loop system is equal or lower than when the pole location are not restricted.

For the guaranteed damping, we choose $\beta = 1$ and a radius $r = 3000$ for the disc. Thus, the combined LMI region becomes

$$\{s \in \mathbb{C} | Re(s) < -1, |s| < 3000\}.$$

4. RESULTS

The optimization results in this section are found using Yalmip (Löfberg (2004)) which is an optimization toolbox in MATLAB. The optimization problems can be solved with different solvers. For each result it is indicated which solver has been used.

In the results below, the disc LMI region is not included since it causes the solvers to be more susceptible to numerical problems.

4.1 Performance loss due to LMI regions

As stated above, the use of the LMI regions comes with a loss of performance. Optimizing the controller for the nominal system does not cause numerical problems when the LMI regions are not considered. Therefore, controller optimization for a nominal plant can serve as an assessment for the performance loss due to the LMI regions. Using the guaranteed damping, the H_2 norm of the system is 5.49 (Mosek) times higher. But as an effect, the condition number of P decreases from $4.6 \cdot 10^{11}$ to $3.7 \cdot 10^9$ (Mosek).

4.2 Vertex enumeration method

In order to gain insight in the importance of individual parameters and what the expected result would be, the vertex enumeration method proposed by Kianfar and Fredriksson (2011) can be used. For this investigation, we use k_1, k_2, d_1, d_2 and m_2 as free plant parameters. Note that m_1 is not considered since the system dynamics mainly depend on ratios the system parameters and not so much of the absolute values of the parameters. Hence, m_1 serves as an anchor for the absolute values of the system parameters. Since five plant parameters are considered, the plant parameter polytope has 32 vertices. The parameter range $\alpha \in [-0.5, 1.0]$ is used, meaning that the plant parameters are allowed to range between half and two times its nominal values. When the H_2-optimal performance is compared at the vertices of the parameter polytope, it appears that a number of vertices have a comparable performance and that the optimal performance is shared by eight vertices. The results for these eight vertices are shown in Table 2.

The common factor for these vertices is that k_2 is at its maximum value and m_2 at its minimum. The eight results are all possible permutations of the parameters with k_2 at its maximum value and m_2 at its minimum. Thus, we can conclude that the parameters k_1, d_1 and d_2 have little influence on the closed loop system performance.

4.3 Plant and controller co-optimization

In light of the results from the vertex enumeration method, we will only use the plant parameters k_2 and m_2 as

k_1	k_2	d_1	d_2	m_2	$\gamma/\gamma_{nominal}$
-	+	-	-	-	0.062466
-	+	-	+	-	0.062464
-	+	+	-	-	0.062466
-	+	+	+	-	0.062464
+	+	-	-	-	0.062471
+	+	-	+	-	0.062470
+	+	+	-	-	0.062471
+	+	+	+	-	0.062470

Table 2. Best performance vertices as found with the enumeration method. (+ represents the maximum parameter value and - represents the minimal parameter value)

optimization variables for the plant and controller co-optimization.

For this problem, the used LMI solvers have trouble solving the convexified LMI problems. The solvers either run into numerical problems or do not find a feasible solution. These numerical problems prevent the iterative optimization from approaching a stationary solution in the optimization space. It is important to note that for every iteration, a feasible plant and controller combination can be found with a performance that is at least equal or better than the performance of the system obtained in the previous iteration. This is guaranteed since the previous result is by design a solution for the current optimization.

It often occurs that the solvers find a result that has lower performance than the result of the previous iteration. At each iteration the solvers try to get as close as possible to the optimal solution of the convexified LMIs but numerical issues may cause the solvers to terminate with a solution that correspond to a system with a sub-optimal performance.

Although a monotonous increase in performance is in theory guaranteed, sub-optimal optimization solutions cause problems. Therefore, we will use the additional constraint

$$\gamma_k \leq \gamma_{k-1}. \tag{32}$$

Furthermore, the solvers may run into numerical issues before a feasible solution to the problem is found. Therefore, if a solver fails to find a feasible solution, another solver is employed. As the default solver we use Mosek. If it fails, we try to find a solution with in order Sedumi, sdpt3 and LMIlab. If none of the solvers is able to find a feasible solution, the co-optimization algorithm is terminated.

The results of the plant and controller co-optimization are given below. Figures 2, 3 and 4 show how the system output, the plant parameters and the controller power develop during the iterative system optimization.

If we compare Figure 2 with Figure 3 we observe that there is still a performance increase when α_{k_2} and α_{m_2} have already reached their bound. The performance improvement is then accounted for by finding improved controller parameters. At the point where the co-optimization is terminated, the controller is not at its optimal parameters as is also reflected in the partial utilization of the available controller power.

If the solvers were able to keep finding feasible solutions to the convexified formulation, the controller is expected to approach a locally optimal controller. Since the plant parameters have already reached its bounds, we can also find a globally optimal controller for this optimal plant. The optimization is terminated after the 88^{th}, for which the relative performance is $\frac{\gamma_{88}}{\gamma_0} = 9.4 \cdot 10^{-2}$. If we consider the system found at the 88^{th} iteration, i.e. α_{88}, and optimize for an H_2 optimal controller we find $\frac{\gamma}{\gamma_0} = 6.2 \cdot 10^{-2}$.

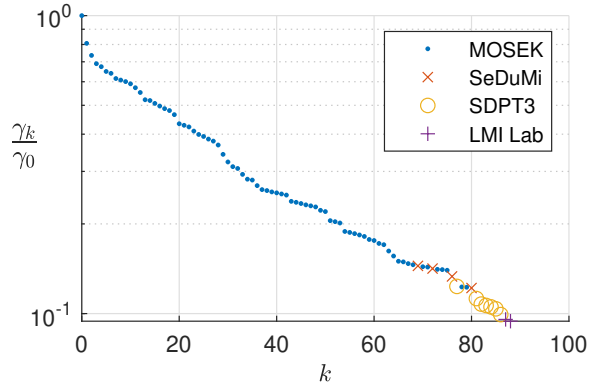

Fig. 2. Asymptotic output covariance during the plant and controller co-optimization relative to the H_2-optimally controlled nominal system.

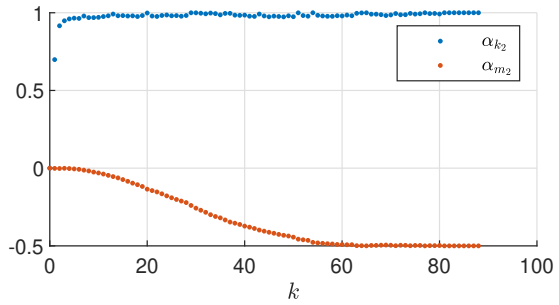

Fig. 3. Development of the parameter weights during the plant and controller co-optimization.

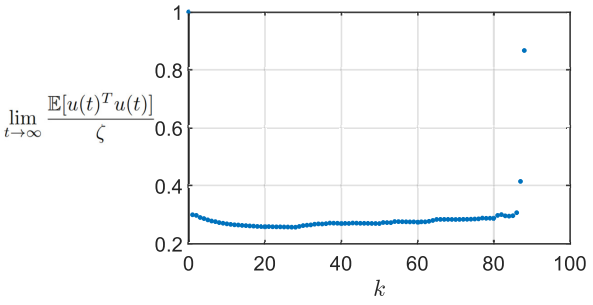

Fig. 4. Power of the control signal relative to the maximally available controller power.

Figure 5 shows the power spectral densities from the disturbances to the internal deformation for the nominal open-loop, the H_2-optimal controlled closed-loop nominal system and the co-optimized closed loop system. The results are quite similar for the nominal closed loop system

and the co-optimized system, but the co-optimized system has an improved attenuation for the full spectrum of the ground vibrations. Furthermore, the co-optimized system has slightly more attenuation for the low-frequency range of the direct disturbance but the voltage noise is less attenuated on the whole spectrum.

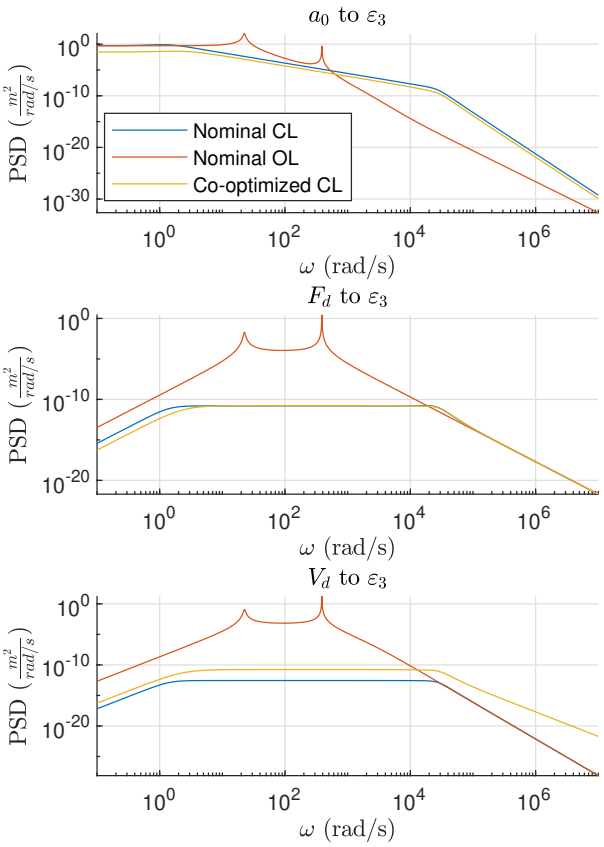

Fig. 5. Power spectral density of the noise sources to the internal deformation.

5. DISCUSSION

As discussed in the results, imposing a guaranteed damping improves the numerics of the optimization problem. Without this LMI region, an H_2-optimal controller can be calculated for the nominal plant but the plant and controller co-optimization algorithm fails at the first iteration. The implementation of this LMI region causes a considerable performance loss, but enables several iterations for the co-optimization algorithm.

It turns out that the used model and constraints do not yield the most insightful example for the iterative algorithm. In this case study, the result of the co-optimization could have been found relatively easy using the vertex enumeration method. However, there are situations for which the vertex enumeration method does not find the optimal solution (see Appendix B for an example). Furthermore, the vertex enumeration method has shown that only few plant parameters have a significant influence on the performance of the closed-loop system.

In theory, the iterative algorithm can run indefinitely unless a stopping logic is applied. This is possible since the solution of the previous iteration is by design also a feasible solution to the current iteration. In this case study, none of the used solvers is able to find a feasible solution at the 89^{th} iteration and thus the iterative algorithm is terminated at this iteration. Furthermore, if at each step of the iterative algorithm the optimal solution is found, the output will vary monotonically to the the optimal solution for the plant and controller co-optimization. For the case study, the used solvers run into numerical problems and cannot find the optimal solution. In order to ensure the monotonicity of the co-optimization, the additional constraint that the new performance should be at least as good as the previous performance is necessary.

Since we did not approach a stationary solution, we do not know whether the found plant parameters belong to the local optimum. However, in this case we know from the results of the vertex enumeration method that the resulting plant parameters are globally optimal.

As for the results of the co-optimization, k_2 is maximized and m_2 is minimized. The maximization of k_2 is to be expected since this stiffens the internal mode and thus suppresses the internal deformation. The minimized mass m_2 may be explained by a more effective use of the controller power since less power is needed to control a smaller mass. A lower value for m_2 also increases the eigenfrequency of the internal deformation, but there is no clear sign in Figure 5 that the disturbance attenuation of the co-optimized system is benefiting from an increased eigenfrequency of the internal deformation.

Numerical precision is found to be the limiting factor for the plant and controller co-optimization. The solvers used in this work rely on double-precision floating point operations. There exist solvers, although less available, that rely on quadruple precision floating point operations. The extra precision may probably be not enough for the co-optimization algorithm to run indefinitely but it may help the co-optimization algorithm to approach a stationary point.

For this case study, a simplified model is used. Namely, we assume that every state can be measured without noise, only a static state feedback controller is considered and the assumption is made that the spectra of the disturbances are flat. In a more realistic case study, not all states are measurable, and measurable states will be measured with noise. A next step would therefore be to consider output feedback with measurement noise and non-flat noise spectra for the disturbances.

6. CONCLUSIONS

This paper presents an iterative algorithm to simultaneously optimize a plant and power-constrained H_2 static state feedback controller while imposing pole placement constraints. This method uses convexified LMI formulations for the plant and controller co-optimization. Convexified LMI formulations for placement of poles within an origin-centered disc and to the left of a vertical line are

developed in this paper. Numerical conditioning is needed in order to run the co-optimization algorithm. Inputs and outputs are rescaled, a balanced realization and pole placement constraints are used for numerical conditioning. The pole placement constraints are effective for the numerical conditioning but come at the cost of performance loss for the closed loop system. With an application to a simplified AVIS, the co-optimization algorithm has shown to yield improved systems, but numerical problems cause the co-optimization algorithm to terminate early, before a locally optimal plant and controller are found.

REFERENCES

Boyd, S. and Barratt, C. (1991). *Linear controller design: limits of performance*. Prentice Hall International Series in Industrial and Systems. Prentice Hall.

Camino, J., Oliveira, M., and Skelton, R. (2003). "Convexifying" linear matrix inequality methods for integrating structure and control design. *Journal of Structural Engineering*, 129.

Caverly, R.J. and Forbes, J.R. (2021). LMI properties and applications in systems, stability, and control theory.

Chen, M., Shen, Y., Majji, M., and Skelton, R. (2023). Integrated economic sensor/actuator selection and covariance control for tensegrity robots —preprint—.

Dettori, M. (2001). *LMI Techniques for control - with application to a compact disc player mechanism*. Ph.D. thesis.

Fathy, H., Reyer, J., Papalambros, P., and Ulsov, A. (2001). On the coupling between the plant and controller optimization problems. In *Proceedings of the 2001 American Control Conference*, volume 3, 1864–1869 vol.3.

Goyal, R., Majji, M., and Skelton, R.E. (2021). Integrating structure, information architecture and control design: application to tensegrity systems. *Mechanical Systems and Signal Processing*, 161, 107913.

Goyal, R. and Skelton, R.E. (2019). Joint optimization of plant, controller, and sensor/actuator design. In *2019 American Control Conference (ACC)*, 1507–1512.

Heertjes, M., Butler, H., Dirkx, N., van der Meulen, S., Ahlawat, R., O'Brien, K., Simonelli, J., Teng, K.T., and Zhao, Y. (2020). Control of wafer scanners: methods and developments. In *2020 American Control Conference (ACC)*, 3686–3703.

Hiramoto, K. and Grigoriadis, K.M. (2006). Integrated design of structural and control systems with a homotopy like iterative method. *International Journal of Control*, 79(9), 1062–1073.

Kajiwara, I. and Nagamatsu, A. (1999). Integrated design of structure and control system considering performance and stability. In *Proceedings of the 1999 IEEE International Conference on Control Applications*, volume 1, 86–91. IEEE.

Kianfar, R. and Fredriksson, J. (2011). Towards integrated design of plant/controller with application in mechatronics systems. volume 7.

Kim, J.H., Shimomura, T., and Okubo, H. (2005). Simultaneous optimal design of structural and control systems via successive LMI optimization. *Journal of Intelligent Material Systems and Structures*, 16(11-12), 977–982.

Löfberg, J. (2004). Yalmip : a toolbox for modeling and optimization in matlab. In *In Proceedings of the CACSD Conference*. Taipei, Taiwan.

Matichard, F., Lantz, B., Mittleman, R., Mason, K., Kissel, J., Abbott, B., Biscans, S., McIver, J., et al. (2015). Seismic isolation of advanced LIGO: review of strategy, instrumentation and performance. *Classical and Quantum Gravity*, 32(18), 185003.

Oliveira, M., Camino, J., and Skelton, R. (2000). A convexifying algorithm for the design of structured linear controllers. volume 3, 2781 – 2786 vol.3.

Roos, F. (2007). *Towards a methodology for integrated design of mechatronic servo systems*. Ph.D. thesis.

Scherer, C. and Weiland, S. (2011). *Linear matrix inequalities in control*. CRC Press.

Shimomura, T. and Fujii, T. (2000). Multiobjective control design via successive over-bounding of quadratic terms. In *Proceedings of the 39th IEEE Conference on Decision and Control*, volume 3, 2763–2768 vol.3.

Shin, Y.H., Moon, S.J., Kim, Y.J., and Oh, K.Y. (2020). Vibration control of scanning electron microscopes with experimental approaches for performance enhancement. *Sensors*, 20(8).

Skelton, R., Iwasaki, T., and Grigoriadis, K. (2017). *A unified algebraic approach to linear control design*.

Spanjer, S. and Hakvoort, W. (2022). Optimal active vibration isolation system design using constrained H_2 control. *IFAC-PapersOnLine*, 55(27), 160–165. 9th IFAC Symposium on Mechatronic Systems 2022.

Van der Poel, T. (2010). *An exploration of active hard mount vibration isolation for precision equipment*. Ph.D. thesis.

Van der Veen, G., Langelaar, M., Van der Meulen, S., Laro, D., Aangenent, W., and Van Keulen, F. (2017). Integrating topology optimization in precision motion system design for optimal closed-loop control performance. *Mechatronics*, 47, 1–13.

Veen, G., Langelaar, M., and Keulen, F. (2014). Integrated topology and controller optimization of motion systems in the frequency domain. *Structural and Multidisciplinary Optimization*, 51.

Appendix A. MULTI-ACTUATOR FORMULATIONS

When considering a power constraint on the controller signal there are two options. Namely, a the combined power of all actuators can be constrained, which may be useful in case of a limited power supply such as a battery. The other option is to constrain the power of each individual actuator, which is useful when, for example, a thermal limit is applicable for individual actuators. A combination of these two options is also possible.

With the first option, the traces in $\lim_{t\to\infty}\mathbb{E}[u(t)^T u(t)] \leq \mathrm{Tr}(KPK^T) = \mathrm{Tr}(FP^{-1}F^T)$ cannot be neglected. By introducing an auxiliary matrix U such that $\lim_{t\to\infty}\mathbb{E}[u(t)^T u(t)] \leq \mathrm{Tr}(KPK^T) = \mathrm{Tr}(FP^{-1}F^T) < \mathrm{Tr}(U)$, we can replace (6b) in Theorem 1 with

$$\begin{bmatrix} U & F \\ F^T & P \end{bmatrix} \succ 0, \tag{A.1a}$$

$$\mathrm{Tr}(U) < \zeta. \tag{A.1b}$$

And we can replace (12b) in Theorem 3 by

$$\begin{bmatrix} U & K \\ K^T & Q \end{bmatrix} \succ 0, \tag{A.2a}$$

$$\mathrm{Tr}(U) < \zeta. \tag{A.2b}$$

For the second option, we need to separate the controller signals. We do that by noting that, with the presence of n actuators, the feedback matrix can be written as

$$K = \begin{bmatrix} K_1 \\ \vdots \\ K_n \end{bmatrix}. \tag{A.3}$$

Consequently, we have

$$F = \begin{bmatrix} F_1 \\ \vdots \\ F_n \end{bmatrix} = \begin{bmatrix} K_1 \\ \vdots \\ K_n \end{bmatrix} P. \tag{A.4}$$

Considering actuator i with power constraint ζ_i, we can then replace (6b) in Theorem 1 with

$$\begin{bmatrix} \zeta_i & F_i \\ F_i^T & P \end{bmatrix} \succ 0, \ \forall i \in \{1, \cdots, n\}. \tag{A.5}$$

And, we can replace (12b) in Theorem 3 by

$$\begin{bmatrix} \zeta_i & K_i \\ K_i^T & P \end{bmatrix} \succ 0, \ \forall i \in \{1, \cdots, n\}. \tag{A.6}$$

Appendix B. EXAMPLE NON-MONOTONIC SURFACE

In Camino et al. (2003) a similar problem is solved as in this paper. In short, Camino et al. (2003) optimizes for a plant and controller with minimal controller power but that satisfies certain performance criteria. The model is very similar and the performance criteria bound the allowed displacements and velocity of the masses.

The important difference between this paper and Camino et al. (2003) is that in this paper the optimization is bounded by only one constraint (the controller power) whereas the optimization problem in Camino et al. (2003) is bounded by multiple constraints on displacements and velocities.

If we perform a grid search over the plant parameters k_2 and d_2 for the system of example 1 in Camino et al. (2003). And calculate for each point the minimal controller energy we obtain the surface in Figure B.1. If the vertex enumeration had been used for co-optimization on this problem, it would not have found the optimum since the minimum is not found at one of the vertices of the plant parameter polytope (i.e. the corner points of this surface).

The surface in Figure B.1 can be viewed as two intersecting surfaces. The two surfaces are formed by different constraints. In this example, there are three constraints on mass velocities and three constraints on mass positions. As it turns out, not all constraints are limiting at the same time. The two surface segments are formed due to different sets of limiting constraints.

If there was only one limiting constraint on the plant parameter polytope, the surface is monotonic and the vertex enumeration method can be used to find the optimal

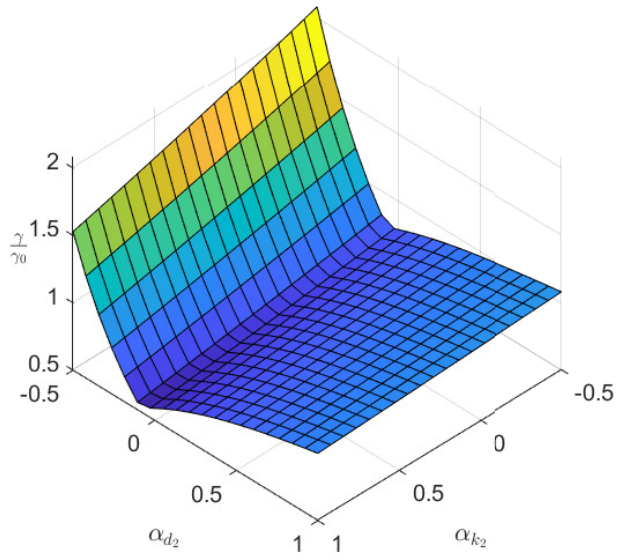

Fig. B.1. Normalized objective of example 1 of Camino et al. (2003). A grid search is performed over parameters d_2 and k_2 and an H_2-optimal controller is calculated at each point.

plant and controller combination at one of the vertices of the plant parameter polytope. This example shows that in the presence of multiple constraints, the surface is not always monotonic and that the vertex enumeration method may fail to find the optimum.

References

Dettori, M. (2001). *LMI Techniques for control - with application to a compact disc player mechanism*. Ph.D. thesis.

Scherer, C. and Weiland, S. (2011). *Linear matrix inequalities in control*. CRC Press.

Skelton, R.E. (2021). *Linear matrix inequality techniques in optimal control*, 1112–1121. Springer International Publishing, Cham.

Van der Poel, T. (2010). *An exploration of active hard mount vibration isolation for precision equipment*. Ph.D. thesis.

A Additional observations

This section contains some observations that contributed to the understanding of the co-optimization algorithm, but not directly to the results in the paper. These observations are unfinished results but could provide useful insights for further research.

A.1 Convexified optimization surfaces

As discussed in the journal paper, numerical problems hinder the iterative algorithm. In general, calculating the initial controller K_0 and P_0 can be accomplished without issues. The numerical problems occur during the iterative part of the plant and controller co-optimization algorithm. Since the optimization problem is highly dimensional and depends on previously obtained solutions, it is hard to obtain a comprehensible overview of the results and detect causes for the numerical issues.

We can, however, study the influence of the system parameters on the convexified optimization problems. This can be done by starting the co-optimization algorithm, but at the first iteration we do not include α_{k_2} and α_{m_2} as optimization parameters. Instead we use these parameters as variables for a grid search. For each pair of α_{k_2} and α_{m_2} we minimize γ subject to (9), (15) and (19) from the journal paper with K and Q as optimization variables. If we then plot the optimal values for γ against α_{k_2} and α_{m_2} we obtain the surface in Figure 3a (LMI Lab). With this surface, we can make a prediction on what values α will obtain from the first iteration with the co-optimization algorithm. Namely, the α for which the parameter dependent surface attains a minimum.

If we take a closer inspection to the parameter dependent surface, we find that not all solutions that have been obtained are a feasible solution to (9), (15) and (19) and thus are invalid solutions. If we filter for the feasible solutions, we obtain Figure 3b, showing holes where the solver did not provide a feasible solution.

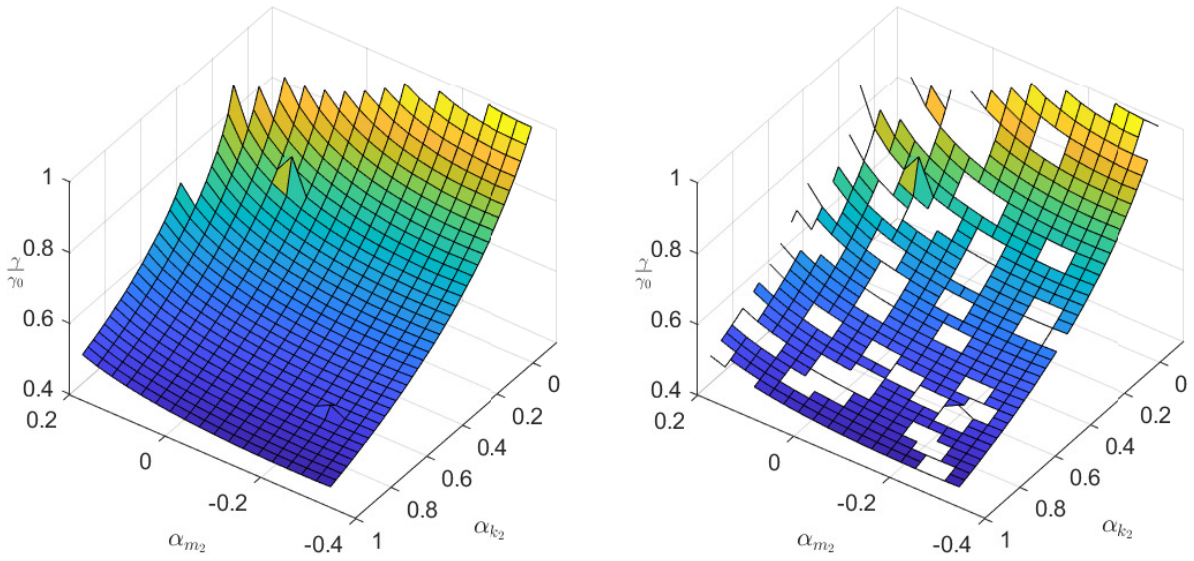

(a) All solutions

(b) Strictly feasible solutions

Figure 3: Grid search over α_{k_2} and α_{m_2} for the first iteration of the co-optimization algorithm. The surface is determined by the optimal output variances resulting for minimization of γ subject to (9), (15) and (19) with K and P as optimization variables. The solutions are obtained with LMI Lab.

The holes in the surface in Figure 3b do not mean that no feasible solution exists for this point but merely that if a feasible solution exists, the solver could not find it and returned the best infeasible solution that has been found before running into numerical problems.

There are no straightforward implications of these holes in this surface but it may prevent the solvers from finding the optimal solution for an iteration and eventually, the co-optimization has to be terminated if none of the solvers find a feasible solution.

The results in Figure 3 are calculated with LMI Lab, which yields the best result. The same grid search does not return any feasible solutions with MOSEK and SeDuMi. SDPT3 only returns a sparse surface of feasible solutions.

A.2 Reduced actuator power

Another observation is that the plant and controller co-optimization algorithm shows a smoother result when the controller is limited to a lower power. If, for example the same problem is considered as in the journal paper but the maximum continuous actuator power is limited to $16 \cdot 10^{-4}$W instead of 16W, we find the co-optimization results as in Figures 4a and 4b. Although the co-optimization algorithm appears to yield smoother results, the algorithm is nonetheless required to terminate when eventually none of the solvers can find a feasible solution. Furthermore, the plant parameters reach their maximum and minimum value relatively quickly after which there is still improvement in the output variance. This improvement of the output variance can then only be caused by improved controllers.

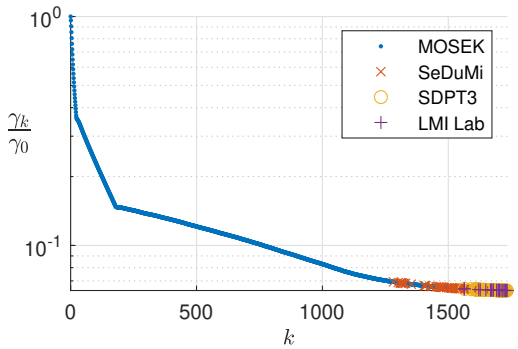

(a) Asymptotic output variance relative to the optimally controlled nominal system during the plant and controller co-optimization.

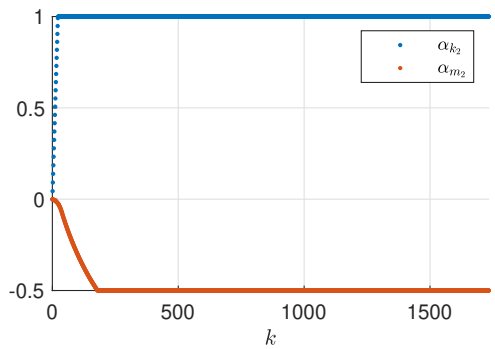

(b) Plant parameter weights during the system and controller co-optimization.

Figure 4: Asymptotic output variance and plant parameter weights during the system and controller co-optimization when the actuator is constrained to a power of $16 \cdot 10^{-4}$W.

A maximum continuous actuator power of $16 \cdot 10^{-4}$W is quite low in comparison to the actual 16W. Figure 5 shows the power spectral densities of the disturbances to the internal deformation. In these plots, the lowered actuator power can be observed by reduced attenuation of the disturbances.

In the case study of the paper we have observed that not all available power is utilized by the controller. Figure 6 shows the utilized controller power during the co-optimization when only $16 \cdot 10^{-4}$W is available for the controller. For this lower-power case, the situation also occurs that not all available power is utilized, but eventually for this case all available power is utilized. This may suggest that the controller is nearer to optimal, but the performance still improves even when all power is already utilized.

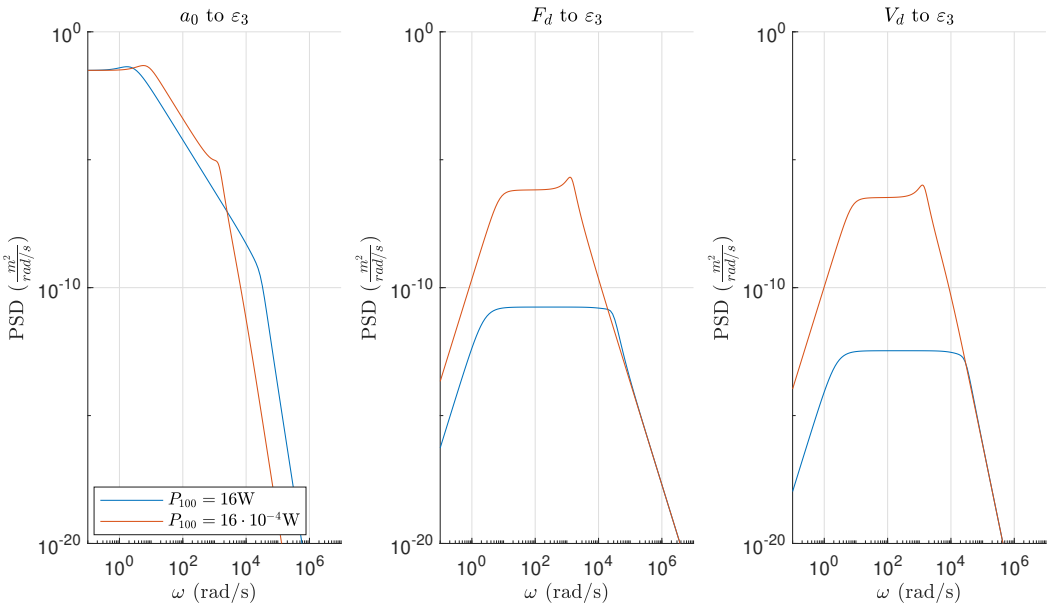

Figure 5: Power spectral densities from the disturbances to the internal deformation for the co-optimized system. The two plots correspond to the co-optimized plant and controller in case the maximum continuous power of the actuator is 16W and $16 \cdot 10^{-4}$W.

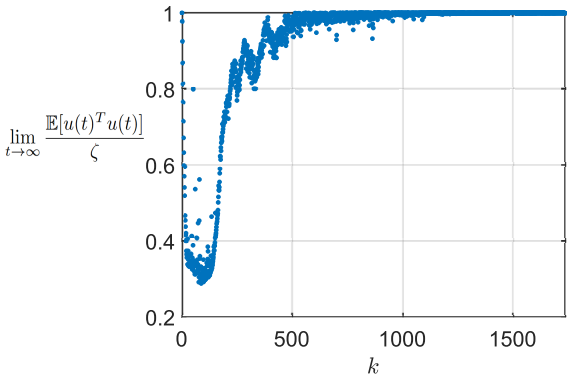

Figure 6: Asymptotic controller power during the iterative co-optimization.